with an anti-sintering agent, PAA-Ca, followed by washing with water.

Figure 7 SEM photograph (a), a TEM photograph (b) and the associated electron diffraction pattern (c) of rod-like HAp crystals calcined at 800°C for 1 h with an anti-sintering agent, PAA-Ca, followed by washing with water.

Figure 8 ATR FT-IR spectra of (a) MOI-oxime monomer, (b) original SF, and (MOI-oxime)-modified SF.

Figure 9 Diffuse reflectance FT-IR spectra of (a) original and (b) (MOI-oxime)-modified calcined HAp nanoparticles.

Figure 10 ATR FT-IR spectra of (a) poly(MPTS) homopolymer, (b) SF fiber, and (c) poly(MPTS)-grafted SF.

Reprinted with permission from [21], T. Furuzono, S. Yasuda, T. Kimura, Si. Kyotani, J. Tanaka and A. Kishida, J. Artif Organis **7**, 137 (2004). © The Official Journal of the Japanese Society for Artificial Organs

Figure 11 ATR FT-IR spectra of (a) poly(MPTS)-grafted SF just after preparation and (b) hydrolyzed poly(MPTS)-grafted SF.

Reprinted with permission from [21], T. Furuzono, S. Yasuda, T. Kimura, Si. Kyotani, J. Tanaka and A. Kishida, J. Artif Organis **7**, 137 (2004). © The Official Journal of the Japanese Society for Artificial Organs

Figure 12 ATR FT-IR spectrum of calcined HAp particles covalently coated on SF fibers.

Reprinted with permission from [21], T. Furuzono, S. Yasuda, T. Kimura, Si. Kyotani, J. Tanaka and A. Kishida, J. Artif Organis **7**, 137 (2004). © The Official Journal of the Japanese Society for Artificial Organs

Figure 13 SEM photograph of calcined HAp nanoparticles covalently coated on an SF fiber.

Reprinted with permission from [21], T. Furuzono, S. Yasuda, T. Kimura, Si. Kyotani, J. Tanaka and A. Kishida, J. Artif Organis **7**, 137 (2004). © The Official Journal of the Japanese Society for Artificial Organs

Figure 14 ATR FT-IR spectra of (a) 4-META monomer, (b) original SF, (c) poly(4-META)-grafted SF, and (d) ionized poly(4-META)-grafted SF.

Figure 15 Difference FT-IR spectrum of diffuse reflectance which subtracts original HAp from HAp nanoparticles with ionized 4-META (——) and FT-IR spectrum of the ionized 4-META monomer (-----) at 1400 – 1330 cm^{-1}.

Figure 16 Mechanical properties of three types of SF fibers (original SF, (MOI-oxime)-grafted SF, and HAp/SF composite fiber). Data were calculated as means of six-time determinations. Error bars represent standard deviations of six-time determinations. ** means an existence of a significant difference ($p < 0.01$) between two samples.

Figure 17 SEM photographs of cell morphologies on (a) gelatin-coated grass, (b) original SF fabric, (c) hydrolysed poly(MPTS)-frafted SF fabric, and (d) calcined HAp nanopartilces covalently coated on an SF fabric.

Reprinted with permission from [21], T. Furuzono, S. Yasuda, T. Kimura, Si. Kyotani, J. Tanaka and A. Kishida, J. Artif Organis 7, 137 (2004). © The Official Journal of the Japanese Society for Artificial Organs

Figure 18 TEM micrograph of cross sectional view of fiber/HAp/cell interface. The stained sample which is fibroblast incubated on HAp/SF for 24h was cut by

microtome.

Reprinted with permission from [21], T. Furuzono, S. Yasuda, T. Kimura, Si. Kyotani, J. Tanaka and A. Kishida, J. Artif Organis 7, 137 (2004). © The Official Journal of the Japanese Society for Artificial Organs

Figure 19 Design of a prototype model of a percutaneous button.

Reprinted with permission from [21], T. Furuzono, S. Yasuda, T. Kimura, Si. Kyotani, J. Tanaka and A. Kishida, J. Artif Organis 7, 137 (2004). © The Official Journal of the Japanese Society for Artificial Organs

Figure 20 External views of the button prototype of a percutaneous device; (a) side view of the button, (b) flexibility of the button, and (c) a silicone tube installed in the button.

Reprinted with permission from [21], T. Furuzono, S. Yasuda, T. Kimura, Si. Kyotani, J. Tanaka and A. Kishida, J. Artif Organis 7, 137 (2004). © The Official Journal of the Japanese Society for Artificial Organs

Figure 21 Magnified view of the edge of the button by SEM observation.

Reprinted with permission from [21], T. Furuzono, S. Yasuda, T. Kimura,

Si. Kyotani, J. Tanaka and A. Kishida, J. Artif Organis 7, 137 (2004). © The Official Journal of the Japanese Society for Artificial Organs

Figure 22 SEM photographs of cell morphologies on the upper views of the button made of (a, b) HAp-coated SF fibers and (c, d) untreated SF fibers. The magnification for (a, c) is x 200 and for (b, d), x 800.

Reprinted with permission from [21], T. Furuzono, S. Yasuda, T. Kimura, Si. Kyotani, J. Tanaka and A. Kishida, J. Artif Organis 7, 137 (2004). © The Official Journal of the Japanese Society for Artificial Organs

Figure 23 External view of the HAp-coated device percutaneously implanted into back of a rabbit for 3 months. The protruding substance is silicone tube, and HAp-coated percutaneous button is implanted just under the epidermis.

Figure 24 SEM and fluorescence photographs of HUVEC adhering on (a, d) original PET, (b, d) collagen-coated PET, and (c, f) HAp/PET compsite.

Figure 25 the images show prototype of an artificial blood vessel made of HAp/PET composite. (a) External view of the prototype. (b, c) lower and higher magnification of SEM images of HAp/PET fibers of inside of the prototype.

(d) Schematic presentation of the reaction process of calcined HAp nanoparticles covalently coated on a PET fiber.

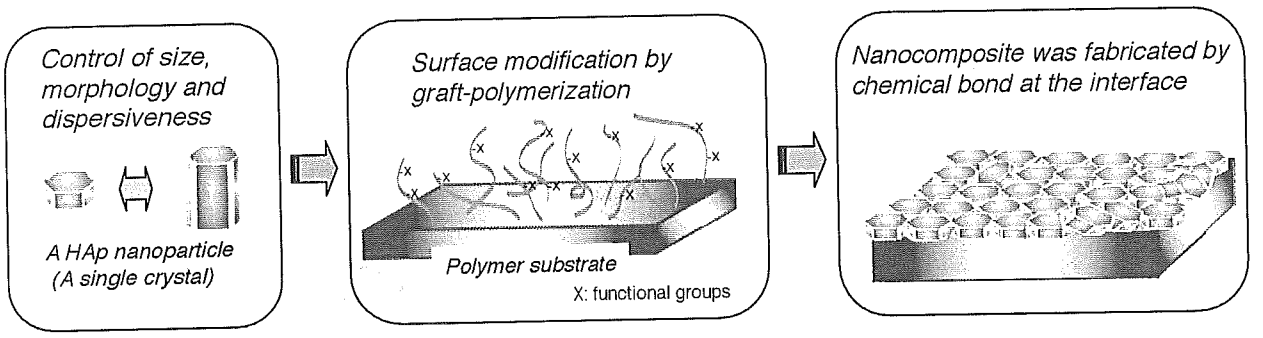

Scheme 1 Furuzono et al.

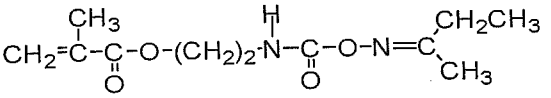

(a) MOI-oxime monomer

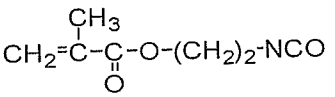

(b) MOI monomer

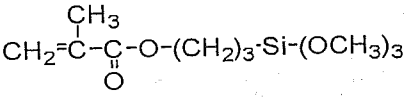

(c) MPTS monomer

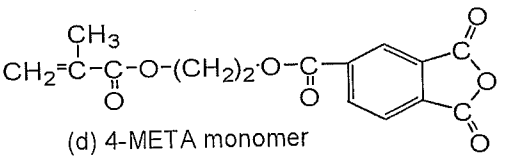

(d) 4-META monomer

Scheme 2 Furuzono et al.

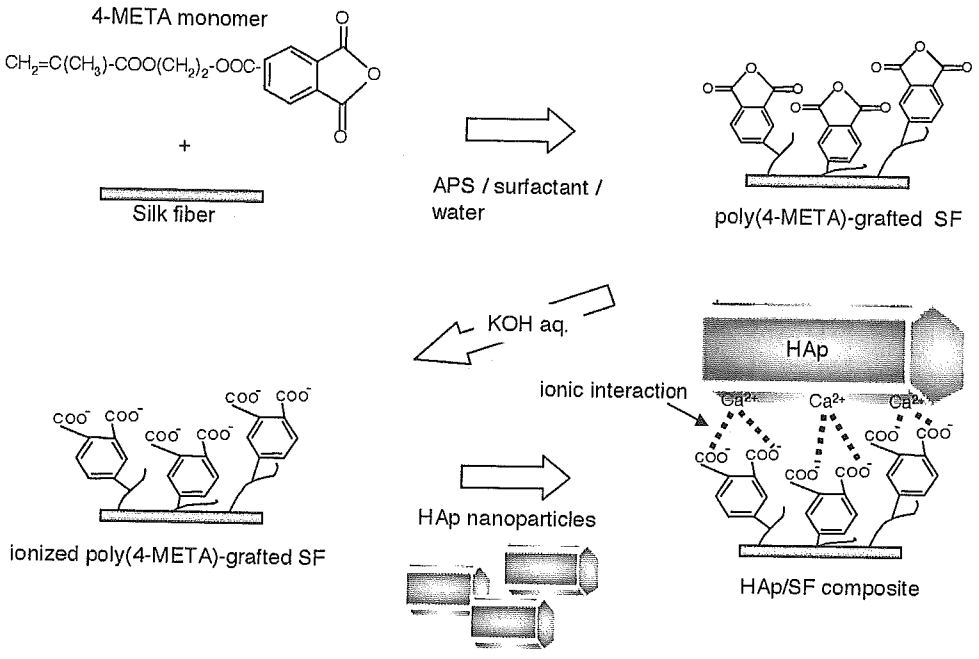

Scheme 3 Furuzono et al.

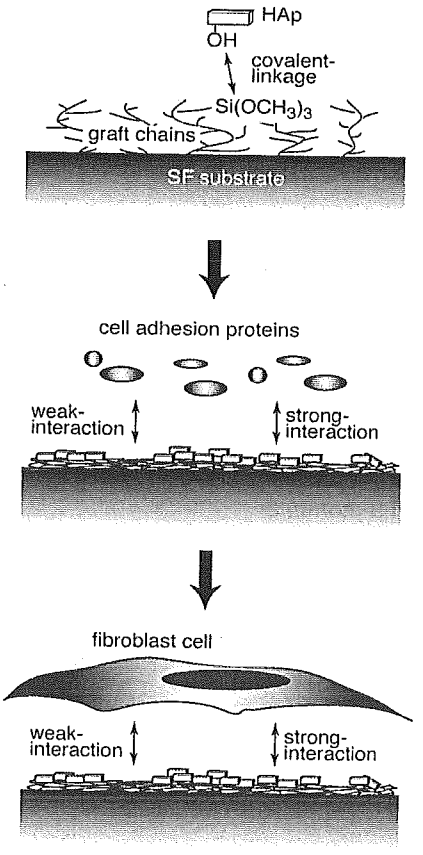

Scheme 4 Furuzono et al.

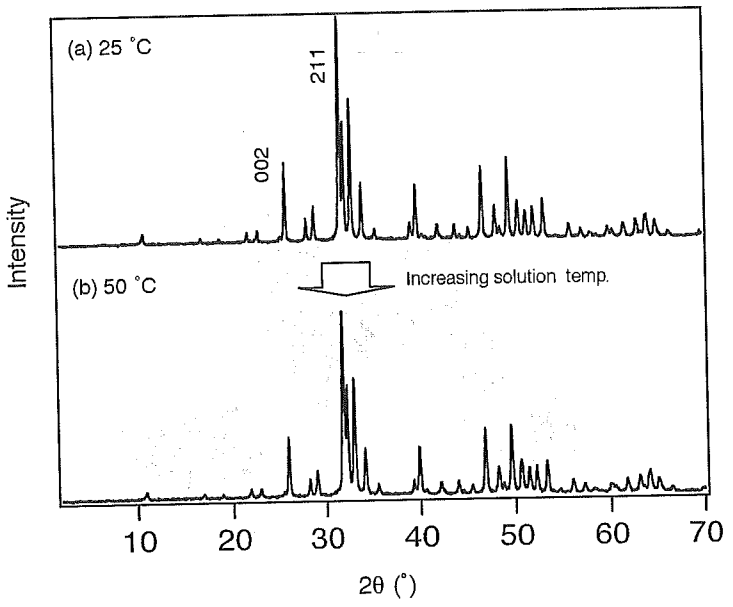

Figure 1 Furuzono et al.

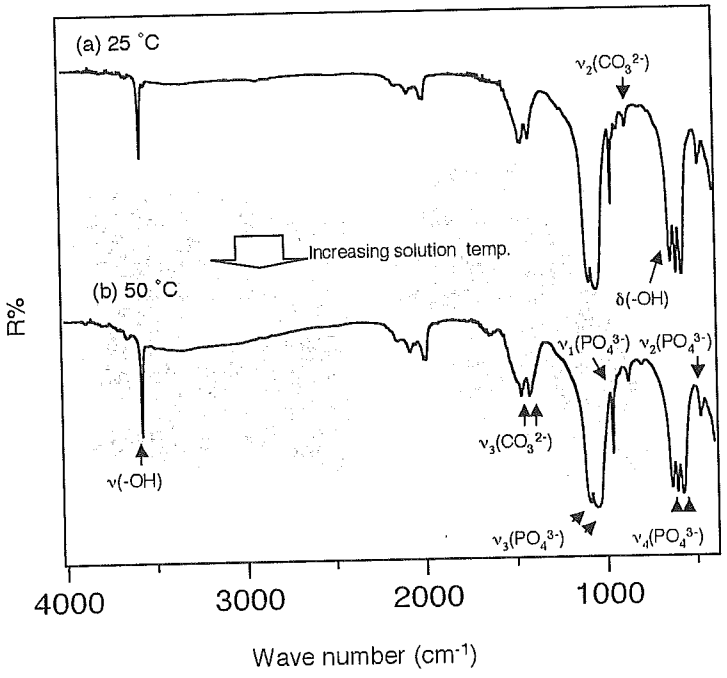

Figure 2 Furuzono et al.

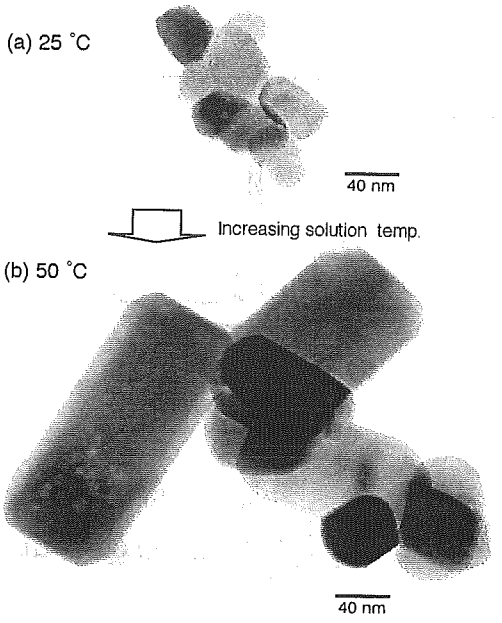

Figure 3 Furuzono et al.

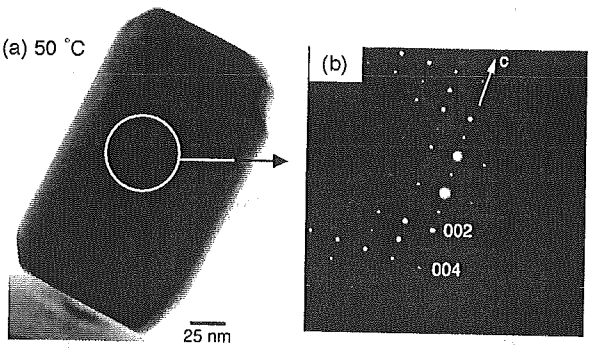

Figure 4 Furuzono et al.

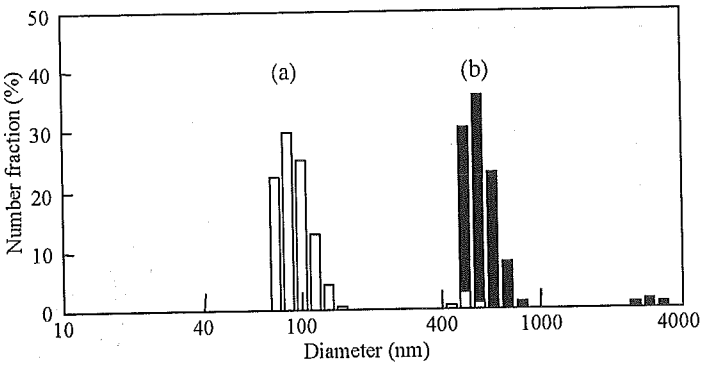

Figure 5 Furuzono et al.

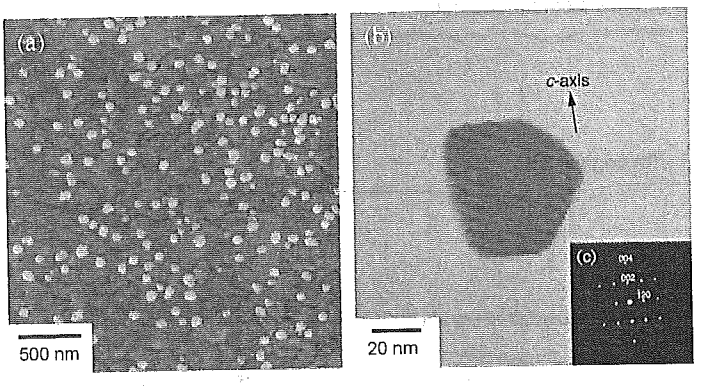

Figure 6 Furuzono et al.

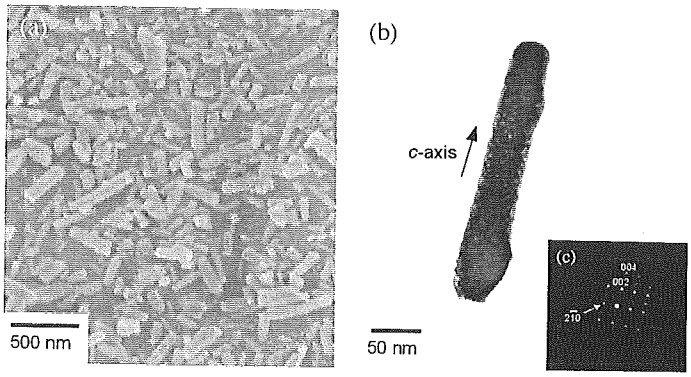

Figure 7 Furuzono et al.

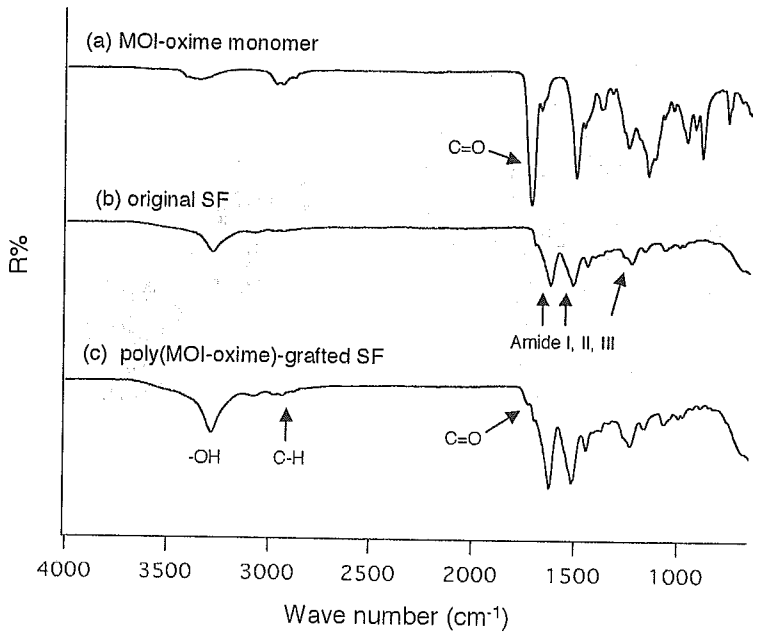

Figure 8 Furuzono et al.

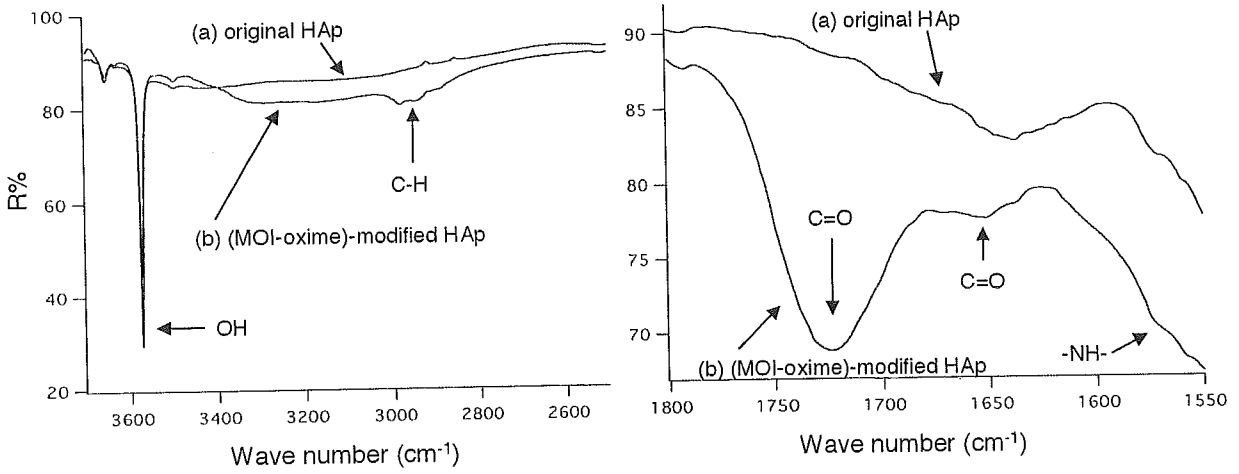

Figure 9 Furuzono et al.

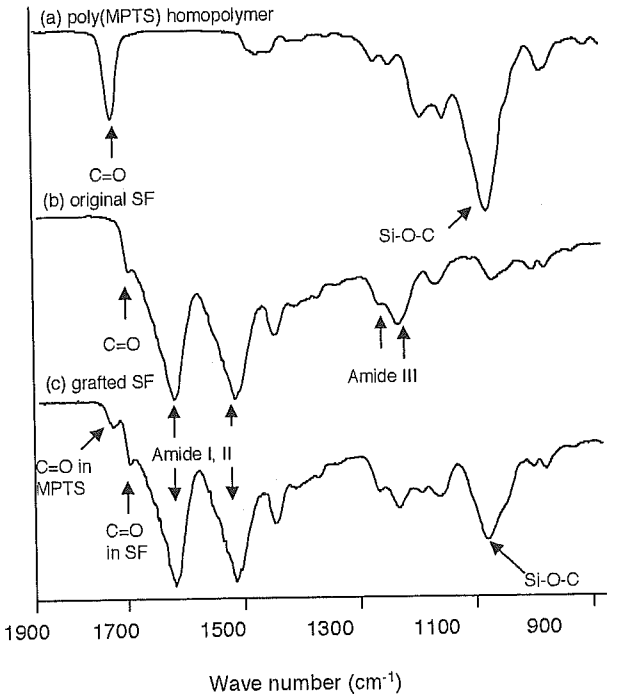

Fig.10 Furuzono et al.

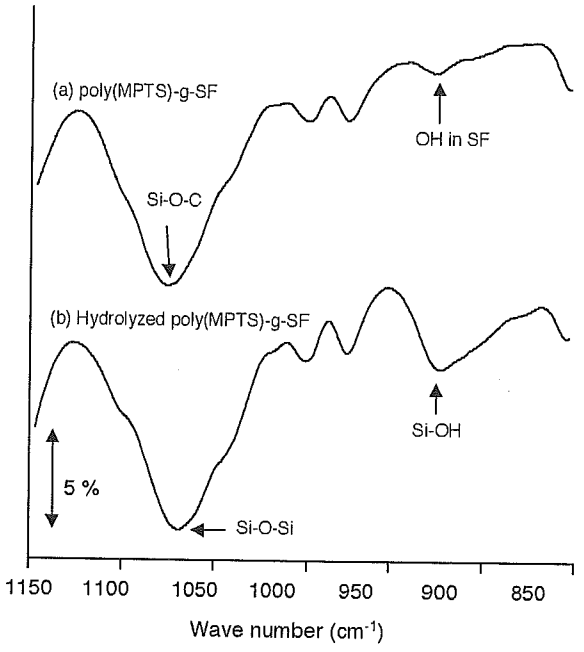

Fig.11 Furuzono et al.

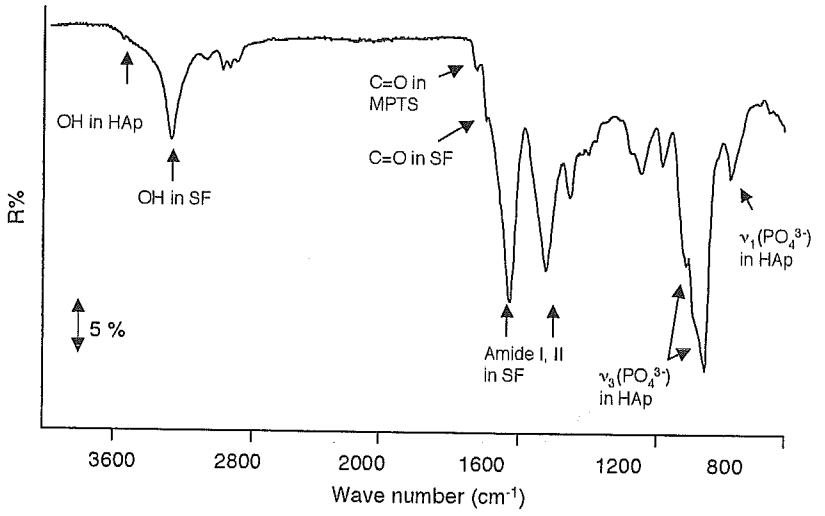

Fig.12 Furuzono et al.

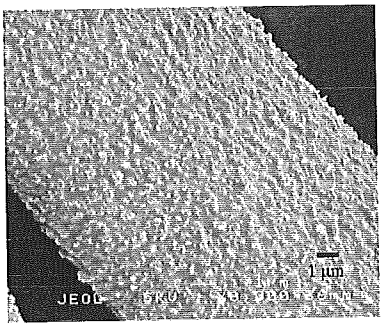

Fig.13 Furuzono et al.

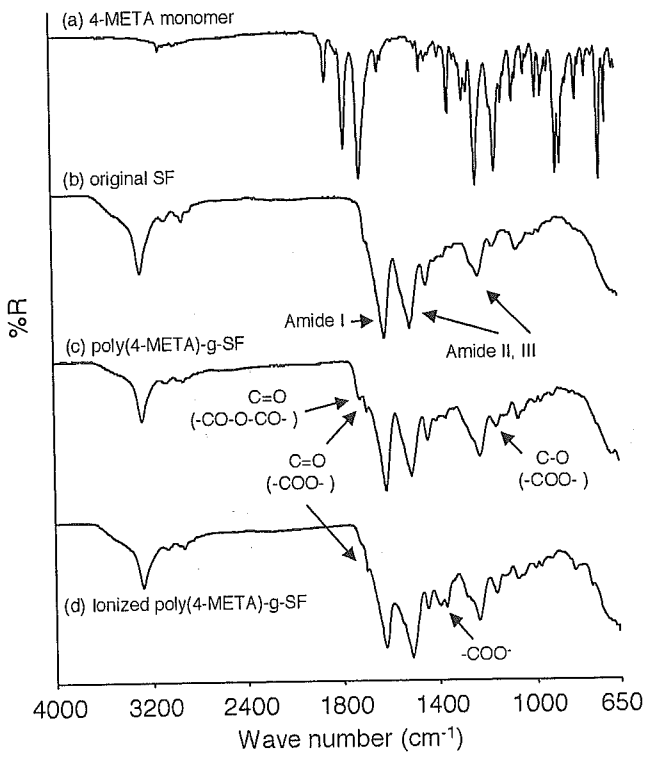

Fig.14 Furuzono et al.

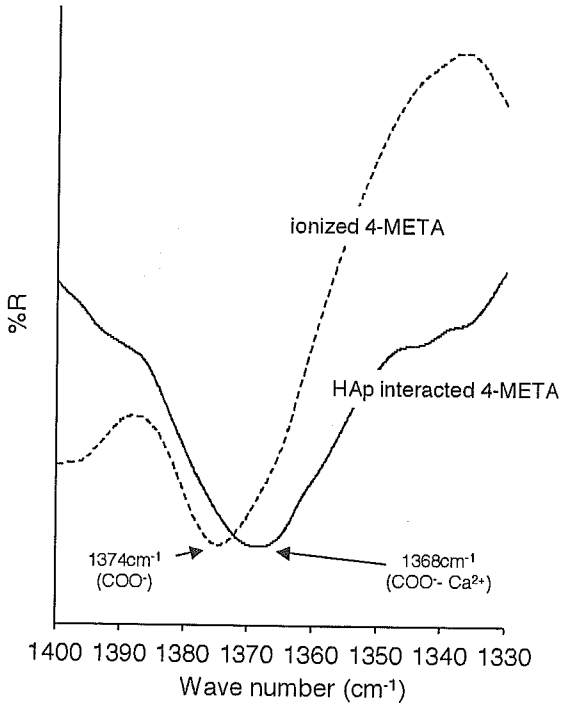

Fig.15 Furuzono et al.

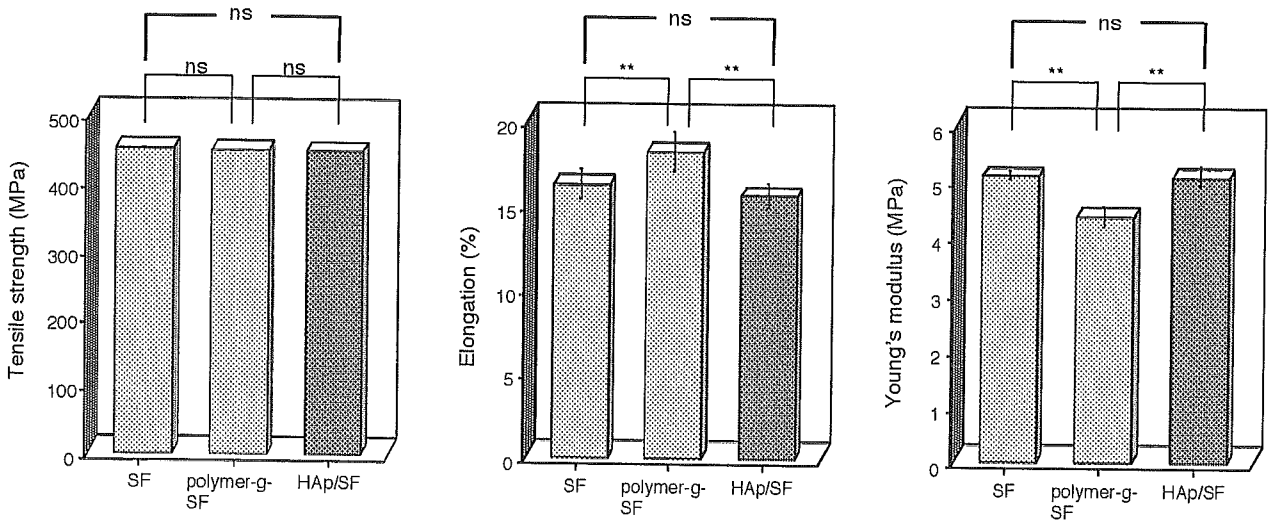

Fig.16 Furuzono et al.

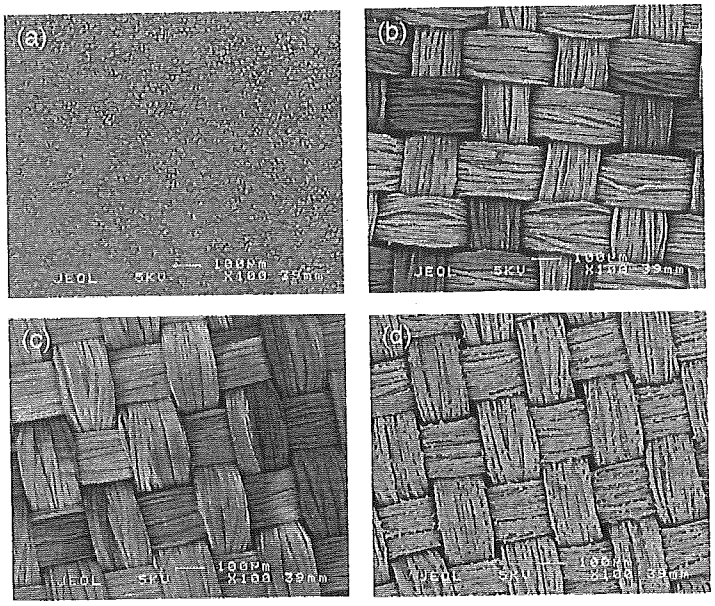

Fig.17 Furuzono et al.

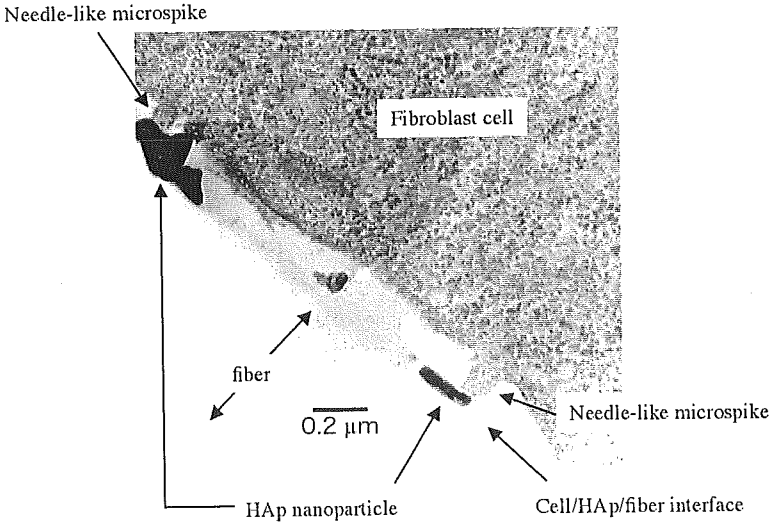

Figure 18 Furuzono et al.

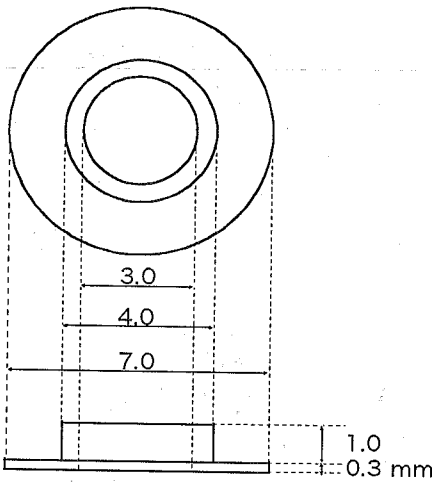

Figure 19 Furuzono et al.

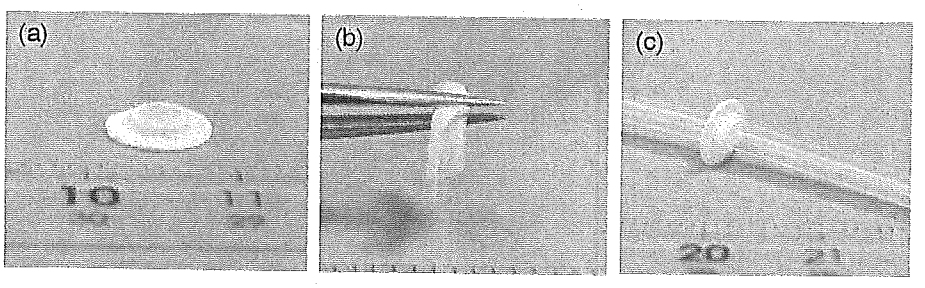

Figure 20 Furuzono et al.

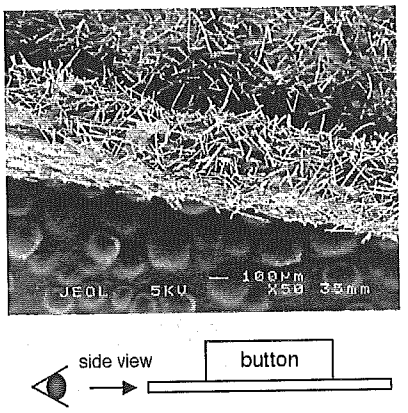

Figure 21 Furuzono et al.

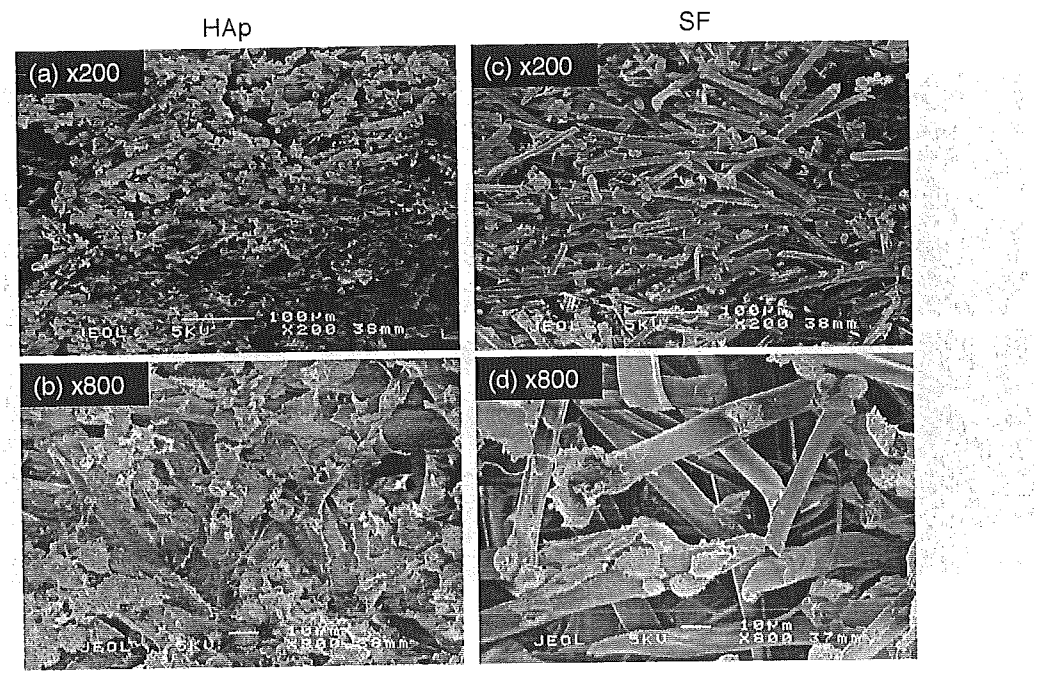

Figure 22 Furuzono et al.

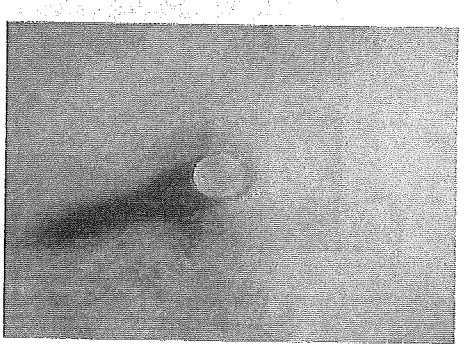

Figure 23 Furuzono et al.

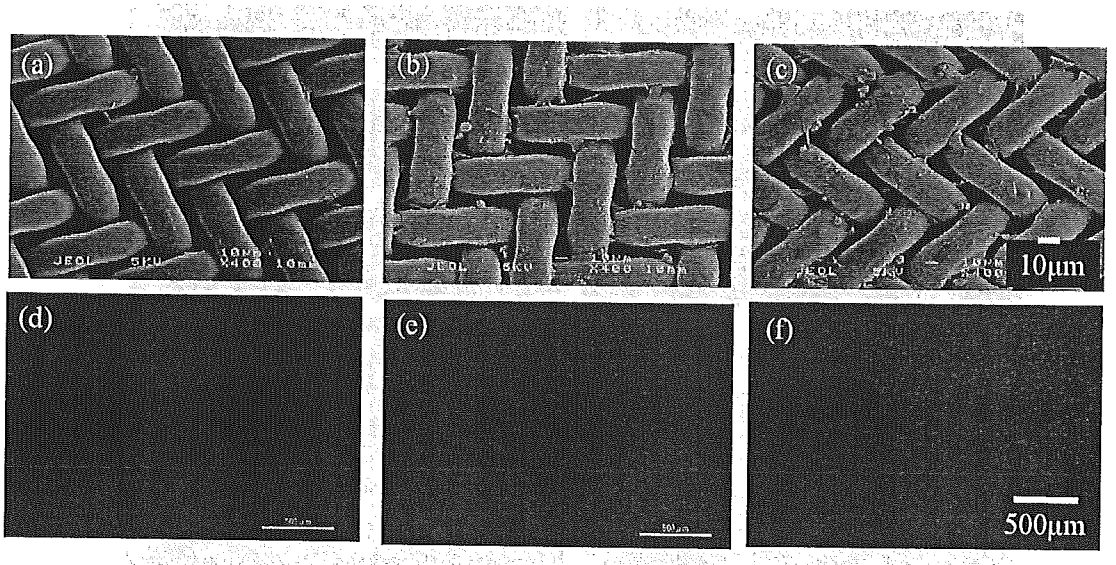

Figure 24 Furuzono et al.